In vivo growth inhibition of head and neck squamous cell carcinoma by the Interferon-inducible gene IFI16. M. DE ANDREA CO-FIRST AUTHOR

In vivo growth inhibition of head and neck squamous cell carcinoma by the Interferon-inducible gene IFI16

Jasenka Mazibrada[a,1], Marco De Andrea[a,b,1], Massimo Rittà[a,b], Cinzia Borgogna[b,] Raffaella dell'Eva[c], Ulrich Pfeffer[c], Luigi Chiusa[d], Marisa Gariglio[b], Santo Landolfo[a]

[a] Department of Public Health and Microbiology, Medical School of Turin, Via Santena 9, 10126 Turin, Italy;

[b] Department of Clinical and Experimental Medicine, Medical School of Novara, Via Solaroli 17, 28100 Novara, Italy;

[c] Functional Genomics National Cancer Research Institute, Largo Rosanna Benzi 10, 16132 Genova, Italy;

[d] Department of Biomedical Sciences and Human Oncology, Medical School of Turin, Via Santena 7, 10126 Turin, Italy

Corresponding author: Prof. Santo Landolfo, Department of Public Health and Microbiology, Medical School of Turin, Via Santena 9, 10126 Turin, Italy; Tel.: +39 011 6705636; fax: +39 011 6705648. E-mail address: santo.landolfo@unito.it.

[1] These two authors contributed equally to this work.

Abstract

The Interferon-inducible gene, IFI16 has been implicated in the control of cell growth, apoptosis, angiogenesis and immunomodulation. In a previous study we demonstrated that restoring levels of IFI16 in a head and neck squamous cell carcinoma (HNSCC)-derived cell line, HNO136, reduced its growth *in vitro* accompanied by a marked increase in doxorubicin-induced apoptosis. To evaluate the ability of IFI16 to inhibit *in vivo* tumorigenesis of HNO136 cells and to characterize the molecular mechanisms responsible for its anti-tumor activity, IFI16 expression on cell growth was evaluated by an *in vivo* tumorigenicity assay. After excision, tumors were subjected to morphometric and immunohistochemical analyses with markers of apoptosis, angiogenesis, and inflammation. Restoring IFI16 expression significantly reduced the *in vivo* tumorigenesis of HNO136, decreased tumor vascularization and increased areas of tumor necrosis. Further analysis revealed that IFI16 expression triggered apoptosis of tumor cells, as evaluated using TUNEL assay. Finally, restoring IFI16 protein to HNO136 cells increased CD45+ inflammatory cell infiltration of the tumor burden, predominantly consisting of CD68/CD14 positive macrophages. In accordance with our previous *in vitro* experiments, this study demonstrates for the first time that IFI16 exerts *in vivo* anti-tumoral activity by promoting apoptosis of tumor cells, by inhibiting neo-vascularisation, and by increasing the recruitment of macrophages through the release of chemotactic factors.

Keywords: Head and neck squamous cell carcinoma; Interferon; IFI16; Growth arrest; *In vivo* tumorigenesis

1. Introduction

The Interferon (IFN)-inducible HIN200 gene family includes a group of human (IFI16, IFIX, MNDA, and AIM2) and mouse (Ifi202a, Ifi202b, Ifi203, Ifi204, and D3/Ifi205) genes [1,2]. The encoded proteins share at least one of three partially conserved repeated motifs with 200-amino acids, A, B, or C. Additionally, some of the proteins in the family, including the IFI16 protein, contain a DAPIN/PYRIN domain in their N-terminus [3,4]. This domain was identified as putative protein-protein interaction domain at the N-terminus of several proteins that are thought to function in apoptotic and inflammatory signalling pathways [5,6]. Of note, HIN200 proteins are primarily nuclear phosphoproteins involved in the transcriptional regulation of genes important for cell-cycle control, differentiation, and immunomodulation [7,8]. This function of the HIN200 proteins may be correlated with the binding and inhibition of several transcription factors, including c-Fos, c-Jun, E2F1, NF-κB, MyoD, c-Myc, and SP1 [7,9-11].

Since its original cloning, IFI16 was initially detected in human lymphoid cells [12,13]. However, further investigation demonstrated that in normal human adult tissues, it is expressed in a highly restricted pattern. It is only present in selected cells within certain organs. Prominent IFI16 expression is seen in stratified squamous epithelia, and it is particularly intense in basal cells of the proliferating compartment, while it gradually decreases in the more differentiated suprabasal compartment. In addition, all vascular endothelial cells from both blood and lymph vessels strongly expressed IFI16, suggesting a possible link to angiogenesis and inflammation [14,15]. Another line of evidence showing that IFI16 is involved in cell stress signalling has been illustrated in cells exposed to oxidative stress. We have found that H_2O_2, S-nitroso-N-acetylpenicillamice (SNAP), and tert-butyl hydroperoxide (TBPH) can up-regulate IFI16 expression in primary human umbilical vein endothelial cells (HUVEC). This change in IFI16 levels in turn activates p53 as shown by increased expression of p53-inducible genes [16]. Consistent with these findings, overexpression of IFI16 in HUVEC efficiently suppressed tube

morphogenesis *in vitro*, which was accompanied by increased expression of proinflammatory molecules [17]. In agreement with a role for IFI16 as a proinflammatory protein, anti-IFI16 autoantibody titres are significantly elevated in patients with autoimmune diseases such as cutaneous systemic sclerosis (lcSSc), systemic lupus erithematosus (SLE), and Sjogren's syndrome (SjS) [18]. Increased levels of IFI16 are indeed correlated with triggering of proinflammatory molecules and cell death by apoptosis, providing further support for the idea that IFI16 could be an important mediator of the chronic inflammation and vascular involvement in systemic autoimmune diseases [19].

Evidence is also accumulating to link IFI16 with control of tumorigenesis. IFI16 has been isolated both as a molecule that is differentially regulated by the p210 BCR/ABL1 fusion oncogene in a cDNA microarray [20] and as a BRCA1-associated protein involved in the p53-mediated apoptosis pathway [3]. A role for IFI16 in commitment to growth arrest or apoptosis under conditions of DNA damage induced by ionizing radiation or doxorubicin treatment has been recently demonstrated [21,22]. Moreover, overexpression of IFI16 inhibited growth and tumorigenicity of both osteosarcoma and chondrosarcoma cells and sensitized them to senescence accompanied by an increase of p21WAF1 and a decrease in the levels of cyclin E, cyclin D1, c-Myc, and Ras [23]. In accordance with these findings, increased levels of IFI16 in prostate epithelial cells contributed to senescence-associated irreversible cell growth arrest and inhibited the colony formation capability of prostate cancer cell lines lacking IFI16 [24]. Finally, immunohistochemical analysis of IFI16 expression in a series of primary head and neck squamous cell carcinomas (HNSCCs) revealed a strong correlation between IFI16 expression levels and tumor histopathologic grade. Sustained IFI16 immunoreactivity was present in low-grade, less aggressive tumors, while IFI16 was barely detectable or negative in high-grade, more aggressive tumors [25]. Thus, the lower proliferation rate of IFI16 strongly-positive tumors may be related to the anti-proliferative activity of the HIN200 proteins.

In this study, we wished to gain further insight into the tumor suppressor activity of IFI16. For this purpose, we restored IFI16 expression in the HNSCC-derived cell line, HNO136, and analyzed its growth properties in nude mice. We demonstrate that restoring IFI16 expression in the head and neck tumor-derived cell lines negative for IFI16, significantly reduces their proliferation and clonogenic activity *in vitro*. Additionally, reduced IFI16 expression diminishes their capability to generate tumors *in vivo*. Moreover, we show for the first time that the tumor suppressor activity of this protein appears to somewhat correlate *in vivo* with IFI16 proinflammatory, proapoptotic, and anti-angiogenic activities.

2. Materials and methods

2.1. Cell culture, cell growth, and soft agar assay

Parental and stable, retrovirally transduced HNO136 cells, produced as previously described [21], were cultured in Dulbecco's modified Eagle's medium (DMEM; Sigma-Aldrich, Milan, Italy) supplemented with 10% heat-inactivated fetal bovine serum (FBS; Sigma-Aldrich) at 37°C and 5% CO_2. Mouse macrophage cell line RAW 264.7, purchased from American Type Culture Collection, was cultured in medium containing RPMI 1640 (Sigma-Aldrich), 10% FBS, and penicillin/streptomycin mix (final concentration: penicillin, 100 IU/mL; streptomycin, 100 μg/mL).

Cell growth in a monolayer was evaluated by the MTT (3-(4,5-dimethylthiazolyl-2)-2,5-diphenyltetrazolium bromide) assay, as previously described [26]. Cells were plated in triplicate at a density of 15,000 cells/well in 24-well cell culture plates. Cells were allowed to adhere overnight and, at the indicated time points, cell growth was measured with the MTT assay. Briefly, 60 μL of MTT (5 mg/mL in PBS) were added to the medium for 4 hours. Medium and

MTT were then removed, dimethyl sulfoxide was added, and absorbance was measured at 570 nm.

Anchorage-independent cell growth was determined by analyzing the formation of colonies in soft agar. Pools of stable cell lines were harvested and aliquots were added to 60-mm dishes containing 0.5% (w/v) SeaPlaque agarose (Cambrex Bio Science) in complete medium on top of a layer of 1% (w/v) SeaPlaque agarose. Aliquots of 1000, 3,000, and 10,000 cells were plated in triplicate. After 14 days of culture, colonies were photographed and counted with the Gel Doc XR documentation system (Bio-Rad Laboratories, Milan, Italy).

2.2. Western blotting analysis

Whole cell protein extracts were prepared as previously described [16]. Briefly, proteins were separated using sodium dodecyle sulfate polyacrylamide gel elecrophoresis (SDS-PAGE) and an 8.5% gel. Proteins were than transferred to a polyvinylidene difluoride membrane (Millipore, Bedford, MA), according to the instruction manual. Filters were blocked overnight in 5% w/v low-fat dry milk in 10mM Tris-HCl, pH 7.5, 0.1 M NaCl and 0.1% Tween-20 and incubated with affinity-purified anti-IFI16 rabbit polyclonal antibody and an actin antibody. Immunocomplexes were detected with appropriate secondary antibodies conjugated to horseradish peroxidase (Sigma-Aldrich) and visualised by enhanced chemiluminescence (SuperSignal, Pierce, Rockford, IL).

2.3. Xenografts

Seven-week-old nude nu/nu (CD-1) mice (Charles River) were used. Each mouse was inoculated by s.c. injection of $5x10^6$ HNO136 cells mixed with liquid Matrigel (final volume 250µl). This cell dose was chosen because was the lowest dose that gave 100% of tumor growth

with parental null HNO136 cells. Tumor size was examined three times per week, and palpable tumors were measured on two perpendicular axes. Tumor volume was calculated by assuming a spherical shape. All animal experiments were conducted in accordance with current national regulations and guidelines for the care and use of laboratory animals (D.L. 27/01/1992, n.116). After 27 days, a total of 19 tumors (nine from mice inoculated with HNO136-neo cells and ten from mice inoculated with HNO136-IFI16 cells), with the volumes ranging between 0.24 mm^3 and 2057 mm^3 were harvested, weighed, and prepared for histopathological and immunohistochemical processing.

2.4. Histopathological and morphometric analysis

Excised tumors were fixed in 4% buffered formalin and embedded in paraffin. The tissue sections were processed for routine histological examinations, stained with haematoxylin eosin, and examined with a light microscope to determine histology. Then, the morphometric analysis was performed by an automated image analyser connected to a Zeiss-Axioscope microscope, using the Image Pro Plus Software (Media Cybernetics, Silver Spring, MD). The following parameters were calculated: numerical density of independent necrotic areas, size (surface area of necrosis in the histological section), and volume density, which refers to the total volume occupied by necrosis in the compartment of the tumor tissue examined.

2.5. TUNEL assay

Apoptosis was evaluated by the In Situ Cell Detection Kit, AP (Roche Diagnostics GmbH, Mannheim, Germany). The cells undergoing apoptotic changes were detected using the terminal deoxynucleotidyl-transferase-mediated dUTP-biotin nick end-labelling (TUNEL) assay, according to the manufacturer's recommendations. Five fields (0.135mm^2 fields at x200

magnification) were selected at random, and the apoptotic index of each field was calculated as a percent of TUNEL-positive cells on the tumor tissue section.

2.6. Immunohistochemical analysis

The following primary anti-sera were used: IFI16 (rabbit polyclonal, working dilution 1:800, generated as described in Gariglio et al. [14]); Ki67 (DAKO Cytomation, Denmark; clone MIB-1, mouse monoclonal, working dilution 1:100); $p16^{INK4a}$ (NeoMarkers, Fremont, CA, USA; clone16P07, mouse monoclonal, working dilution 1:50); CD34 (BioLegend, San Diego, CA, USA; clone MEC14.7, rat monoclonal, working dilution 1:100); CD45 (Caltag Laboratories, Burlingame, CA, USA; clone 30-F11, working dilution 1:50); CD68 (Imgenex, San Diego, CA, USA; clone KP1, working dilution 1:50), and CD14 (BD Biosciences, Milan, Italy; clone rmC5-3, working dilution 1:100).

Serial sections, 4 μm thick, were cut from each selected block, deparaffinised, and then rehydrated. For most of the markers analyzed, antigen unmasking was performed by microwaving in a conventional pressure cooker, where the slides were placed for 30 minutes in 10mM citrate buffer at pH 6.0 (or Tris 10mmol/L, EDTA 1mmol/L at pH 9.0 for CD34).

Endogenous-peroxidase activity was blocked with 3% hydrogen peroxide solution in 1x PBS. Slides were incubated sequentially with Protein Blocking Agent (Ultratech HRP Streptavidin_Biotin Universal Detection System, Immunotech, Marseille, France) to reduce non-specific binding.

Afterwards, the slides were incubated with the primary antibodies for 1 hour at room temperature in a humid chamber or overnight at 4°C for CD34 and CD45 antibodies. The biotinylated secondary antibody was then applied to the slides, followed by incubation with streptavidin-horseradish peroxidise complex (Immunotech, Marseille, France). As a negative control, the appropriate slides were incubated with 1xPBS instead of the primary antibody. The

immunologic reactions were developed at room temperature with 3'3'-diamino-benzidine tetrahydrochloride solution (Roche, Mannheim, Germany), counterstained with Mayer's Haematoxylin, dehydrated, and finally mounted with EUKITT (Bio-Optica, Milan, Italy).

2.7. Interpretation of immunohistochemical staining

Ki67 and p16INK4a expression was evaluated by determining the percentage of squamous cells showing nuclear immunoreactivity for Ki67 and nuclear and/or cytoplasmic staining for p16INK4a. As IFI16 positive cells expressed equally intensive nuclear staining without observable nucleolar reactivity, IFI16 immunoreactivity was expressed as a percentage of the positive cells showing nuclear staining. Immunohistochemical stains for CD45, CD68 and CD14 were interpreted semiquantitatively by assessing the intensity and the extent of staining for the entire tissue section presented on the slide. First, the total percentage of positively staining tumor cells was determined, and the extent of staining was assessed using a five-grade scale: grade 0 (1-10% of positive cells on the tissue section), grade 1 (11-25% positive cells), grade 2 (26-50% positive cells), grade 3 (51-75% positive cells) and grade 4 (76-100% positive cells). The percentage of weakly (1), moderately (2), and strongly (3) staining cells was determined, so that the sum of these categories was equal to the overall percentage of positive cells. A staining score was then calculated as follows: score (out of maximum of 12) = sum of 1 x grade for extent of weak, 2 x grade for extent of moderate, and 3 x grade for extent of strong staining. Immunostaining was scored as described above in at least five high-power fields of tumor specimens. The mean value of the two independent counts by two observers was considered the final value. Slight differences in interpretation were resolved by simultaneous analysis.

2.8. Microvessel density (MVD) assessment

According to the principle of the Weidner method, the sections were scanned at a low magnification (40x, 100x), and the most active areas of neovascularisation for the invasive tumor, represent the highest microvessel density (neovascular "hot spot"), were located prior to counting. These steps were performed after endothelial cells lining the microvessels had been highlighted with an anti-CD34 antibody. The number of microvessels in five 400x microscopic high-power fields (hpf) containing the area of greatest neovascularisation within or immediately adjacent to each tumor, was determined. Finally, the mean vessel count of the five hot spots was calculated. Any cells stained brown and morphologically recognized as endothelial cells were considered a microvessel and were counted. In addition, any cluster of endothelial cells with or without (rudimentary or well-formed) lumen were counted as microvessels.

2.9. Chemotaxis assay

For in vitro chemotaxis assay, RAW 264.7 cells, having properties similar to those of mouse resident macrophages and exhibiting responsiveness to chemotactic stimuli [27] were used. Twenty-four hours after plating, supernatants of HNO136-neo or HNO136-IFI16 cells were added to a 24-well tissue culture plate in a volume of 600ul. Wells with medium only were used as a control. A cell culture insert (BD Biosciences) of 5 μm pore size was put into each well and approximately $1x10^6$ macrophages resuspended in 200μl of RPMI1640 medium containing 0.5% BSA were loaded on each insert. The plates were incubated for 4h at 37°C under air containing 5% CO_2. After incubation, the inserts were removed and the cell number in each bottom well was determined with a hemocytometer. The chemotactic index (CI) was calculated from the formula: CI = (number of migrating cells affected by supernatant / number of migrating cells affected by the negative control).

2.10. Statistical analysis

All statistical analyses and graphs were performed using GraphPad Prism version 4.03 for Windows (GraphPad Software, San Diego California USA, www.graphpad.com). The data were presented as the mean value with standard error of the mean (SEM). An unpaired student t-test was used to compare means. Pearson's correlation was applied to evaluate the relationship between two variables with a normal distribution, and Spearman's test was utilized for non-parametric tests. Two-tailed p-values less than 0.05 were considered statistically significant.

3. Results

3.1. IFI16 exerts its growth-inhibitory effect on HNO136 cells in vivo.

We previously reported that restoring IFI16 expression in HNO136 cells, a HNSCC-derived cell line, reduces their growth rate and their ability to be transformed *in vitro* [21, and Supplementary figure 1], thus representing a suitable model to analyze the mechanisms exploited by IFI16 to inhibit tumour growth *in vivo*. We then asked whether cells expressing IFI16 (HNO136-IFI16) would display reduced tumorigenicity in nude mice xenografts. As shown in Fig. 1a, inoculation of *in vitro* transduced cells into nude mice revealed a strong anti-tumorigenic effect of IFI16 expression. Tumor size was examined twice a week, and palpable tumors were measured on two perpendicular axes. Tumor volume was calculated by assuming that the shape was spherical. While cells transduced with control retroviruses (HNO136-neo) and untransduced cells readily formed localized palpable tumors of comparable size (not shown), HNO136-IFI16 cells lost their tumorigenic potential, producing tumors of a significantly smaller size ($p=0.023$ at day 27). At day 27, due to the dramatically increasing tumor size in the control group, the animals were sacrificed. As reported in the scatter dot plot in Fig. 1b, the weight analysis

conducted on excised tumors confirmed that those from IFI16 transduced cells were significantly smaller than controls (p=0.0464).

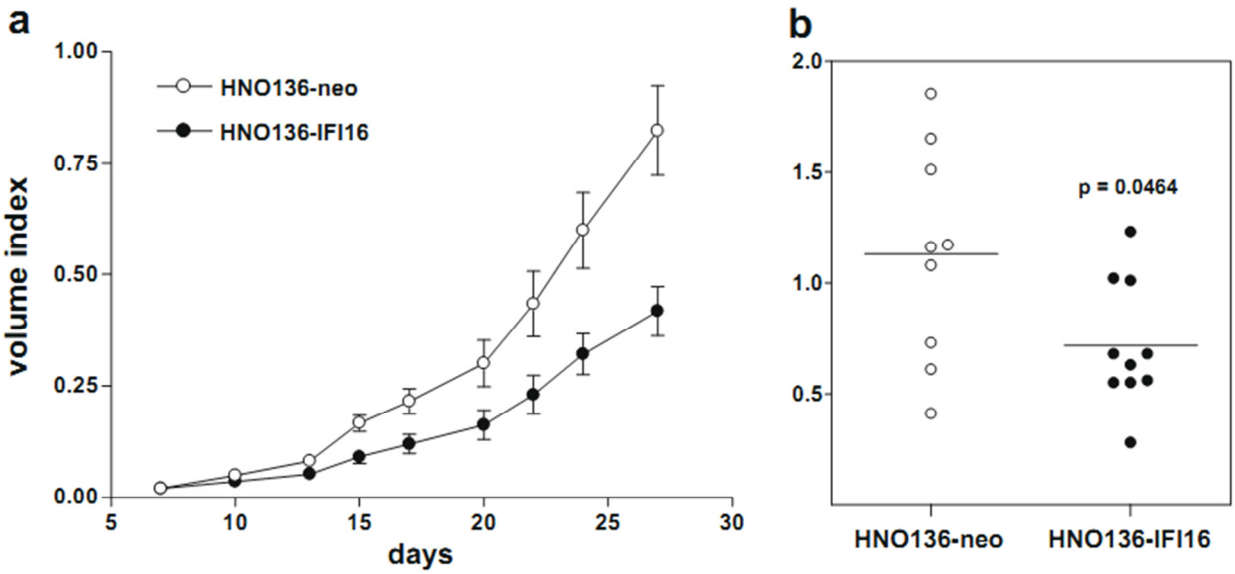

Fig. 1. Decreased tumorigenicity of IFI16 overexpressing HNO136 cells. (a) Tumor growth curves for control (white circles) compared to IFI16 expressing cells (black circles). Differences between groups, starting 15 days after implantation, were highly significant at the time of sacrifice (p = 0.023, day 27). (b) Scatter plot representing tumor weights at day 27. Tumors derived from HNO136 cells expressing IFI16 (black circles) showed a significant reduction in weight compared to control cells (white circles) (p = 0.0464).

3.2. HNO136-IFI16 tumors were smaller and more necrotic than control HNO136 tumors.

To further analyze the characteristics of excised tumors, we performed morphometric analysis, using Image Pro Plus Software, as described in the Material and Methods. As illustrated in Table 1 and reported in Fig. 2, this analysis revealed that the volume of HNO136-IFI16 tumors were significantly reduced when compared to the volume of tumors derived from control cells (p=0.0287). An average tumor volume of 992.1 mm^3 was reported in the group of

HNO136-neo derived neoplasms and 459.9 mm^3 in the neoplasms derived from HNO136-IFI16 cells.

Table 1. Morphometric and immunohistochemical properties of HNO136-arising tumors.

		HNO136-neo		HNO136-IFI16
Tumor volume[a]	Median	770.50		474.20
	Mean ± SEM	992.10 ± 206.60		459.90 ± 101.10
	Range	182.40–2057.00		0.24–1061.00
	p^*		0.0287	
Tumor necrosis[b]	Median	14.80		31.00
	Mean ± SEM	15.03 ± 2.90		33.53 ± 5.34
	Range	1.90–30.90		7.00–63.30
	p^*		0.009	
Apoptosis[b]	Median	20.00		42.50
	Mean ± SEM	16.67 ± 2.89		39.80 ± 3.10
	Range	5.00–30.00		25.00–50.00
	p^*		<0.0001	
IF I16[b]	Median	10.00		50.00
	Mean ± SEM	14.11 ± 2.38		44.20 ± 5.65
	Range	7.00–30.00		15.00–65.00
	p^*		0.0002	
Ki67[b]	Median	70.00		82.50
	Mean ± SEM	68.56 ± 15.49		76.20 ± 18.56
	Range	40.00–87.99		30.00–92.00
	p^*		0.3465	
pl6INK4[b]	Median	95.00		90.00
	Mean ± SEM	84.44 ± 25.79		90.80 ± 8.15
	Range	30.00–100.00		75.00–100.00
	p^*		0.4687	
CD34[b]	Median	16.0		8.70
	Mean ± SEM	15.98 ± 1.05		9.81 ± 0.87
	Range	11.80–22.30		7.00–14.50
	p^*		0.0003	
CD45[b]	Median	4.00		5.50
	Mean ± SEM	3.78 ± 0.22		5.40 ± 0.31
	Range	3.00–5.00		4.00–7.00
	p^*		0.0006	
CD68[c]	Median	3.00		4.00
	Mean ± SEM	2.80 ± 0.249		4.00 ± 0.211
	Range	2.00–4.00		3.00–5.00
	p^*		0.0017	
CD14[d]	Median	3.00		4.50
	Mean ± SEM	2.60 ± 0.267		4.40 ± 0.371
	Range	1.00–4.00		3.00–6.00
	p^*		0.0010	

 Unpaired t-test.

a Results for tumor volume are expresses as mm3.

b Results are expressed as a percentage of positively stained cells.

c Results for CD34 are expressed as a number of positive blood vessels.

d Results for CD45, CD68 and CD14 are expressed as a immunostaining score.

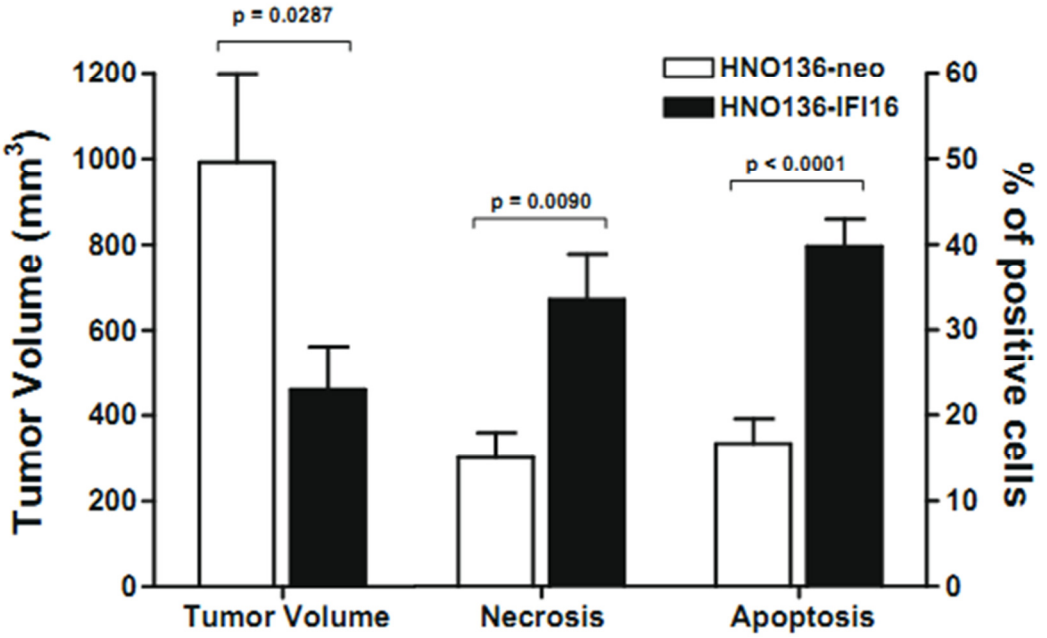

Fig. 2. Morphometric analysis and TUNEL assay. Tumors arising from the HNO136-IFI16 cell lines have markedly reduced volume ($p = 0.0287$), are more necrotic ($p = 0.0090$), and contain a high percent of malignant cells undergoing apoptotic changes ($p < 0.0001$). Means tumor volume expressed in mm3 (cuboid pattern columns, left y-axis), while the percentage of necrotic and apoptotic cells is presented on the right y-axis (black and white columns, respectively).

Examination of hematoxylin-eosin stained sections in both groups of HNO136 tumors revealed the histomorphological features of squamous cell carcinomas without keratinisation, with medium to low differentiation. Gross and microscopic examination of H&E-stained lung and liver tissues from all tumor-bearing mice revealed no signs of micrometastases (data not shown), suggesting that both parental or transduced HNO136 cells are incapable of promoting spontaneous self-dissemination. Necrotic zones were observed, predominantly in the central parts of the tumor sections, but they were also present as independent patchy areas anywhere in the tumor mass, often confluent between them and circumscribed with the inflammatory infiltrate. The volume of necrosis, estimated from the cross sections and obtained as a sum of the

circumscribed necrotic zones, was markedly larger in HNO136-IFI16 tumours (p=0.0090) when compared to the tumours derived from the control cell group. The mean values in HNO136-neo and HNO136-IFI16 were 15.3% (181.2 mm3) and 33.53% (115.4mm3), respectively (Fig. 2). The percentage of cells undergoing apoptotic changes, evaluated by the TUNEL assay, was significantly higher in the HNO136-IFI16 cell line (p<0.0001), which supports the previously observed pro-apoptotic activity of IFI16. This function of IFI16 is also confirmed by the strong positive correlation between the percentage of apoptotic cells and immunohistochemical expression of IFI16 in our specimens (p=0.0010, r^2= 0.4815; Fig. 5b).

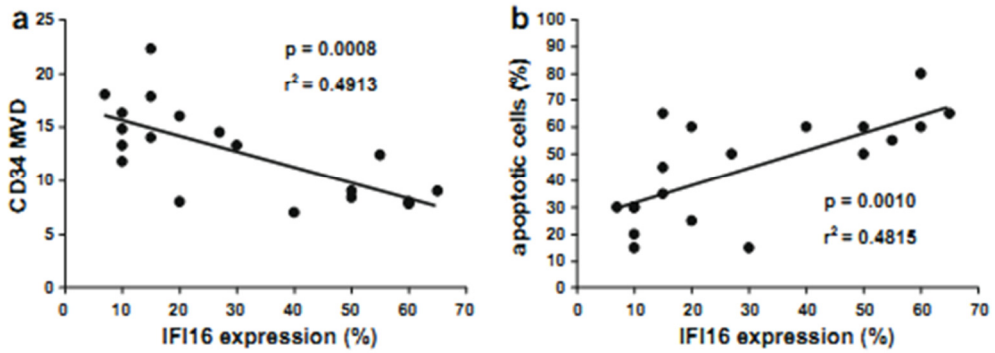

Fig. 5. (a) Correlation of microvessel density as determined by immunohistochemistry with anti-CD34 antibodies in HNO136-neo and HNO136-IFI16 tumors. CD34-MVD showed inverse correlation with IFI16 expression (p = 0.0008, r2 = 0.4913, Pearson's test). The line represents the calculated regression line. (b) Correlation of the percentage of apoptotic cells and cells expressing IFI16. A strong positive correlation was observed (p = 0.0010, r2 = 0.4815, Pearson's test). The line represents the calculated regression line.

3.3. The expression of IFI16 in HNO136-neo and HNO136-IFI16 tumors as determined by immunohistochemistry.

To further clarify the morphological differences observed, we performed a detailed immunohistochemical analysis on paraffin-embedded sections derived from excised tumors.

First, by immunostaining with polyclonal monospecific antibodies, we confirmed the overexpression of IFI16 in tumors from HNO136-IFI16 cells. As seen in Fig. 3a, these tumors expressed high levels of the IFI16 protein, compared to cells derived from HNO136 negative cells.

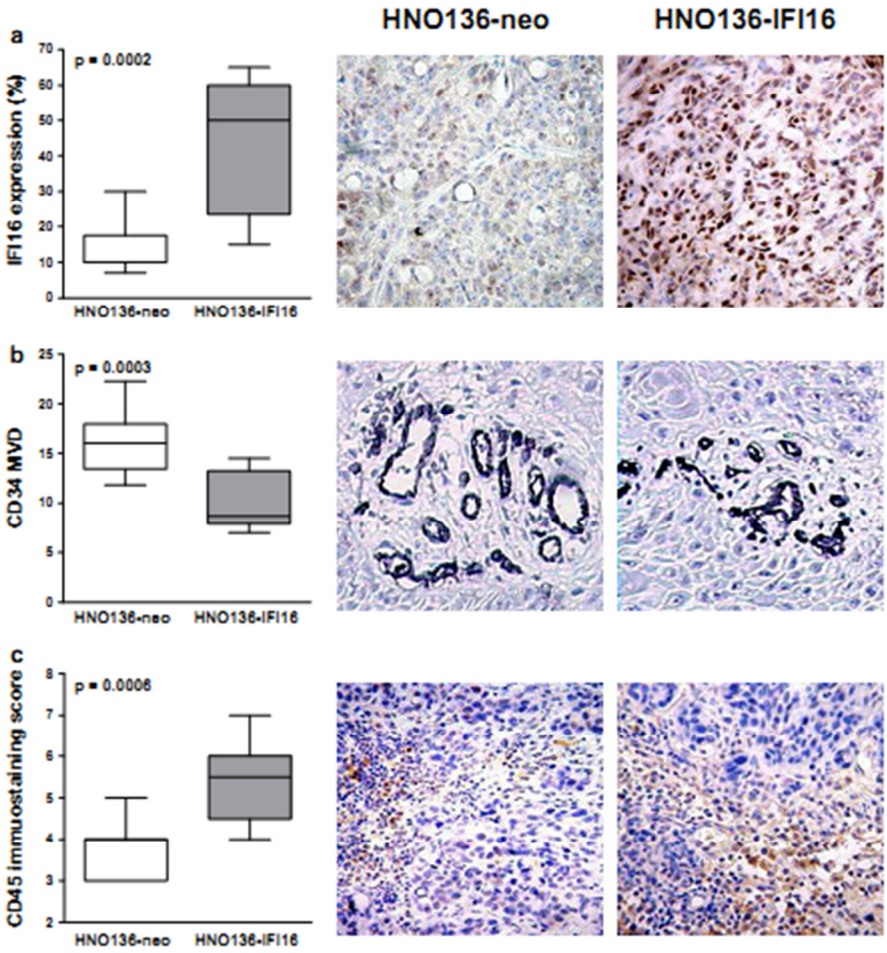

Fig. 3. Immunohistochemical analysis in HNO136-neo and HNO136-IFI16 arising tumors using the following antibodies: anti-IFI16, pan-endothelial marker anti-CD34, and pan-leukocyte marker CD45. (a) IFI16 expression was significantly increased in HNO-IFI16 tumors ($p = 0.0002$), (b) CD34-MVD was significantly reduced in the same tumor group ($p = 0.0003$), (c) with a marked increase in the density of the inflammatory infiltrate ($p = 0.0006$) (immunohistochemical stains with hematoxylin counterstain, original magnification 200×).

After demonstrating that IFI16 overexpression has a significantly negative correlation with tumor masses and a positive one with apoptosis, we looked for markers associated with cell proliferation. Interestingly, immunohistochemical analysis performed with anti-Ki-67 and $p16^{INK4A}$ antibodies revealed that, despite the significantly different volumes of necrotic areas, proliferation markers were expressed at a similar level in the necrotic-free area of the different tumors (Table 1). Although these data seem to be in contrast with the in vitro finding showing inhibition of growth upon IFI16 expression, the possibility exists that in vivo HNO136 cells gradually become resistant to the IFI16 antiproliferative activity. Thus, tumor rejection is afforded by different mechanisms based on the anti-angiogenic and immunomodulatory activity of IFI16.

We previously demonstrated that IFI16 inhibits endothelial cell proliferation and tube morphogenesis *in vitro* [16, 17]. Following this observation and the morphometric analysis described in the previous section, we assessed the capability of IFI16 to impair the angiogenic activity of HNO136 cells by investigating the expression of the neovascularisation marker, CD34. Microvessel density (MVD) was compared in the two tumor groups using the method of Weidner, an international consensus report for angiogenesis counting in solid tumor specimens. The tumors derived from HNO136-IFI16 lines were significantly less vascularised ($p=0.0003$, Fig. 3b), in comparison to those derived from the control group. Consistent with the previously observed anti-angiogenic role of IFI16 during *in vitro* and *in vivo* studies, a negative correlation between CD34-MVD and IFI16 expression was documented in our samples ($p=0.0008$, $r^2=0.4913$, Fig. 5a). In addition, angiogenesis, characterised by immunostaining for CD34, seemed to directly influence the necrotic changes in tissues, as shown by statistical tests ($p=0.0055$, $r^2= 0.3732$).

Previous works from our group and others have pointed towards an important role for IFI16 in immunomodulation and proinflammatory activity [28]. With this scenario in mind, monoclonal antibodies against the pan-leukocyte marker CD45 were used for

immunohistochemistry to look at differences in the expression of this protein between sections from IFI16 positive or negative tumors. A stronger and more diffuse staining was observed for CD45 in HNO136-IFI16 tumors (p=0.0006, Fig. 3c), with a continuous distribution of CD45-positive cells found at the stromal/epithelial junction. Overall, the expression of IFI16 in HNO136 tumors significantly correlated with positive CD45 staining (p=0.0041, r^2=0.3928), with the extension of tissue necrosis (p=0.0444, r Spearman=0.4659), and with the percentage of apoptotic cells (p=0.0444, r Spearman=0.4659), thus proving an *in vivo* role of IFI16 in the proinflammatory response during carcinogenesis.

The observation that IFI16 expression correlates with infiltration of cells positive for the pan-leukocyte CD45 marker, prompted us to assess the chemoattractant activity of supernatants derived from IFI16-overexpressing HNO136 cells and to better characterize the infiltrating leukocyte population responsible for tumor rejection. To this purpose we performed in vitro chemotaxis experiments to assess the capability of HNO136-IFI16 cells to release chemoactrant factors. As shown in Fig. 4a, the supernatants from HNO136-IFI16 cells showed effective chemoattractive activity on mouse macrophages, and the chemotactic index was significantly higher than the values from HNO136-neo cells (6.06 ± 0.42 vs 2.12 ± 0.62). Consistent with this finding we have previously demonstrated that IFI16-overexpressing endothelial cells produce in the supernatant a proinflammatory molecule array polarized to attract cells of the monocyte/macrophage lineage [28, and unpublished data]. Therefore, to better characterize the nature of the infiltrating cells, staining with antibodies against two commonly expressed antigens on macrophages -CD68 and CD14- was performed. Although CD68 and CD14 can both be expressed in macrophages and the precursor monocytes, not all monocytes express both markers concomitantly [29]. Representative images of tumors derived from HNO null cells or HNO overexpressing IFI16 with CD68 or CD14-positive infiltrating macrophages are shown in Fig.4b. The staining signal was located in the membrane and cytoplasm but not in the nucleus. The results of the immunostaining are summarized in Table 1. As shown in Fig. 4b and Fig. 4c,

IFI16-expressing tumors showed dense infiltration by both CD68 and CD14-positive macrophage infiltrate located nearby the necrotic areas of the tumor burden (p=0.0017 and p=0.0010 respectively). By contrast, IFI16 null tumors were found to have sparse or moderate CD68- and CD14-positive macrophage infiltrate. Taken together, these results demonstrate that IFI16 expression leads to tumor rejection by triggering leukocyte infiltration through the release of chemoattractant factors.

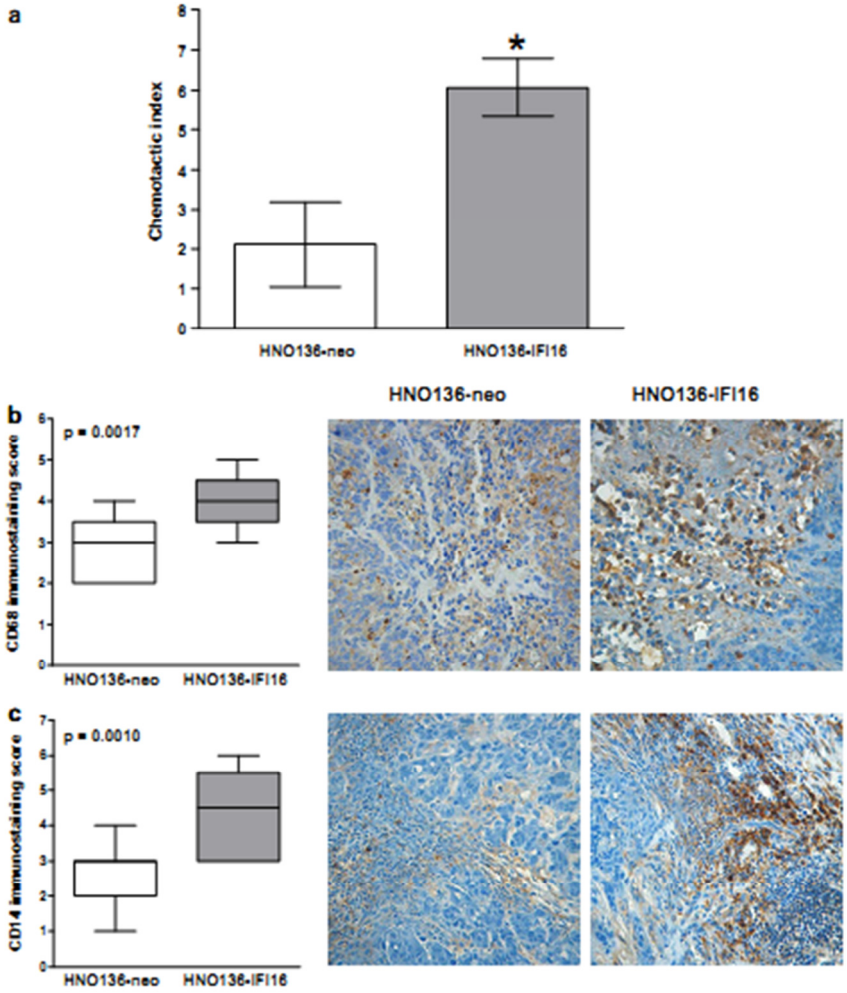

Fig. 4. Characterization of chemoattraction capability of HNO136-IFI16 cells. (a) In vitro chemoattraction was significantly increased by HNO-IFI16 supernatants (*$p < 0.05$, compared to medium control). (b) CD68- and (c) CD14-positive macrophages significantly infiltrate IFI16-expressing tumors ($p = 0.0017$ and $p = 0.0010$, respectively) (immunohistochemical stains with hematoxylin counterstain, original magnification 200×).

4. Discussion

To investigate the role of IFI16 in tumorigenesis of head and neck cancers *in vivo*, we took advantage of a series of HNSCC-derived cell lines with known defects in the pathways regulating cell growth [21]. The HNO136 cell line used in this study displays barely detectable levels of IFI16 even under IFN-stimulation. However, the cell line contains functional p53, which is one of the main regulators of IFI16 activity. This cell line was therefore chosen for reconstitution experiments to assess the antiproliferative activity of IFI16 *in vivo*. Of note, the patient from whom the cell line was derived had a very short period of disease-free survival and died two months after surgery [30], suggesting that the IFI16/p53 pathway may contribute to control tumor growth and differentiation *in vivo*. This hypothesis is now sustained by the finding that restoring IFI16 expression though retroviral transduction, in the presence of wild-type p53, down-regulates HNO136 cell proliferation, decreases HNO136 clonogenic activity *in vitro*, and inhibits tumorigenicity *in vivo*. Altogether, these observations demonstrate that loss or reduction of IFI16 expression correlates with more aggressive HNSCC tumors. In support of this statement, immunohistochemical analysis of IFI16 expression in a series of primary HNSCCs revealed a strong correlation between expression levels and tumor histopathologic grade. Sustained IFI16 immunoreactivity was present in low-grade, less aggressive tumors, while IFI16 was barely detectable or non-existent in high grade, more aggressive tumors [25]. Moreover, restoring IFI16 expression in negative cell lines increased doxorubicin-induced cell death by accumulating cells around the G2/M phase [21]. Consistent with our findings, immunocytochemical and immunohistological analyses of breast cancer cell lines and tumor specimens revealed that levels of IFI16 are frequently decreased, supporting the notion that loss of IFI16 is closely associated with tumor development [31]. Moreover, a role for IFI16 in commitment to growth arrest or apoptosis under conditions of DNA damage induced by ionizing radiation or neocarcinostatin treatment has also been demonstrated [22]. Significantly, forced

expression of IFI16 in prostate cancer lines (LNCaP, PC-3, and DU-145) *in vitro* inhibited cell proliferation, which was associated with upregulation of p21CIP1 expression and a senescence-like phenotype in the PC-3 cell line [32]. In line with these observations, the level of IFI16 was markedly lower in human osteosarcomas when compared with its level in normal bone [23]. Overexpression of functional IFI16 in human osteosarcoma and chondrosarcoma cell lines markedly inhibited colony formation and significantly inhibited cell growth. The decrease in cell growth could be reversed by introducing gene specific siRNA into the tumor cells. Altogether, these results demonstrate that IFI16 is involved in the control of tumorigenesis and in increasing tumor cell sensitivity to cytotoxic drugs. However, since these studies have been conducted predominantly *in vitro*, they do not provide any information about the potential role of IFI16 in suppressing *in vivo* tumor growth and the molecular pathways activated to prevent tumor cell growth.

To address this question, we assessed the ability of IFI16 to inhibit tumor growth *in vivo* by injecting HNO136 cells that have been transduced with an IFI16-expressing retroviral vector into nude mice. The results obtained in this study show for the first time that IFI16 is capable of retarding *in vivo* tumor growth. TUNEL analysis performed on paraffin-embedded tumor samples showed that tumor cells underwent apoptosis *in vivo* upon IFI16 overexpression. Of note, immunohistochemical analysis demonstrates that along with induction of apoptosis, suppression of angiogenesis may be an additional mechanism exploited by IFI16 to impair tumor growth. Immunostaining with an anti-CD34 antibody, a marker of neoangiogenesis, confirms indeed the decrease of vessel density in the tumors produced by IFI16-transduced HNO136 cells. Consistent with these observations, transduction of IFI16 into human endothelial cells efficiently suppressed endothelial migration, invasion, and formation of capillary-like structures *in vitro* [17]. In parallel, sustained IFI16 expression inhibited cell-cycle progression, accompanied by significant induction of p53, p21, and hypophosphorylated pRb [33]. These findings, along with the observation that endothelial cells immortalized by human papillomavirus type 16 E6/E7

oncogenes became resistant to antiangiogenic and anti-proliferative effects of IFI16 overexpression, suggest a relevant role of IFI16 in the p53 transduction pathway [17].

Inflammatory cell infiltration of tumors contributes either positively or negatively to tumor invasion, growth, metastasis, and patient outcomes. These effects are due to tumor heterogeneity and the diversity of the inflammatory cells that infiltrate the tumor mass [34-37]. A stronger and more diffuse staining for anti-CD45 in HNO136-IFI16 tumors was observed when compared to HNO136-null tumors, where CD45-positive cells were primarily found at the stromal/epithelial junction. The increase of infiltrating CD45-positive cells appears to be correlated with the capability of IFI16-expressing HNO cells to release chemoattractant factors in the supernatants. Subsequent immunohistochemical staining revealed that IFI16-positive tumors undergoing rejection contain dense CD68- or CD14-positive monocyte/macrophage infiltrates, likely responsible for inhibition of tumor proliferation in vivo. These results are consistent with our recent findings that IFI16 overexpression in endothelial cells *in vitro* activates the expression of molecules such as ICAM-1, E-selectin, and VCAM and leads to the production of chemokines such as IL-8 and MCP1 [28]. These proinflammatory molecules, in turn, may recruit inflammatory cells that lead to apoptosis and necrosis of the tumor mass, along with growth retardation.

In conclusion, our study demonstrates that IFI16 exhibits strong anti-tumor effects *in vivo* animal models of human HNSCC xenografts by exploiting three main mechanisms, including induction of apoptosis and necrosis in tumor cells, inhibition of angiogenesis, and recruitment of inflammatory cells. These data indicate that IFI16 may serve as a suitable target for therapeutic intervention in tumors of epithelial origin.

Acknowledgements

This work was supported by the following grants: Special Project Oncology "Compagnia di San Paolo", MIUR ("Program 40%" to S.L.), Ricerca Sanitaria Finalizzata 2006 (to M.D.A., M.G. and S.L.), 2007 (to S.L.) and 2008 (to M.G., S.L. and M.D.A.) from Regione Piemonte, and by contributions from the Ministero della Salute (to U.P.). We thank Dr. Christel Herold-Mende for kindly providing the HNO136 cell line. We thank Dr Dusan Lalosevic, Institute of Pathology and Histology, Clinical Centre of Novi Sad, Serbia for helpful discussion.

Conflicts of Interest Statement

The authors declare no conflict of interest for this article.

References

[1] S. Landolfo, M. Gariglio, G. Gribaudo, D. Lembo, The Ifi 200 genes: an emerging family of IFN-inducible genes, Biochimie 80 (1998) 721-728.

[2] L.E. Ludlow, R.W. Johnstone, C.J. Clarke, The HIN-200 family: more than interferon-inducible genes?, Exp. Cell. Res. 308 (2005) 1-17.

[3] J.A. Aglipay, S.W. Lee, S. Okada, N. Fujiuchi, T. Ohtsuka, J.C. Kwak, Y. Wang, R.W. Johnstone, C. Deng, J. Qin, T. Ouchi, A member of the Pyrin family, IFI16, is a novel BRCA1-associated protein involved in the p53-mediated apoptosis pathway, Oncogene 22 (2003) 8931-8938.

[4] K. Dalal, F. Pio, Thermodynamics and stability of the PAAD/DAPIN/PYRIN domain of IFI-16, FEBS Lett. 580 (2006) 3083-3090.

[5] J. Bertin, P.S. DiStefano, The PYRIN domain: a novel motif found in apoptosis and inflammation proteins, Cell Death Differ. 7 (2000) 1273-1274.

[6] N. Inohara, G. Nunez, NODs: intracellular proteins involved in inflammation and apoptosis, Nat. Rev. Immunol. 3 (2003) 371-382.

[7] B. Asefa, K.D. Klarmann, N.G. Copeland, D.J. Gilbert, N.A. Jenkins, J.R. Keller, The interferon-inducible p200 family of proteins: a perspective on their roles in cell cycle regulation and differentiation, Blood Cells Mol. Dis. 32 (2004) 155-167.

[8] R.W. Johnstone, J.A. Trapani, Transcription and growth regulatory functions of the HIN-200 family of proteins, Mol. Cell. Biol. 19 (1999) 5833-5838.

[9] D. Choubey, S.J. Li, B. Datta, J.U. Gutterman, P. Lengyel, Inhibition of E2F-mediated transcription by p202, Embo J. 15 (1996) 5668-5678.

[10] B. Datta, W. Min, S. Burma, P. Lengyel, Increase in p202 expression during skeletal muscle differentiation: inhibition of MyoD protein expression and activity by p202, Mol. Cell. Biol. 18 (1998) 1074-1083.

[11] X.Y. Ma, H. Wang, B. Ding, H. Zhong, S. Ghosh, P. Lengyel, The interferon-inducible p202a protein modulates NF-kappaB activity by inhibiting the binding to DNA of p50/p65 heterodimers and p65 homodimers while enhancing the binding of p50 homodimers, J. Biol. Chem. 278 (2003) 23008-23019.

[12] M.J. Dawson, J.A. Trapani, R.C. Briggs, J.K. Nicholl, G.R. Sutherland, E. Baker, The closely linked genes encoding the myeloid nuclear differentiation antigen (MNDA) and IFI16 exhibit contrasting haemopoietic expression, Immunogenetics 41 (1995) 40-43.

[13] J.A. Trapani, K.A. Browne, M.J. Dawson, R.G. Ramsay, R.L. Eddy, T.B. Show, P.C. White, B. Dupont, A novel gene constitutively expressed in human lymphoid cells is inducible with interferon-gamma in myeloid cells, Immunogenetics 36 (1992) 369-376.

[14] M. Gariglio, B. Azzimonti, M. Pagano, G. Palestro, M. De Andrea, G. Valente, G. Voglino, L. Navino, S. Landolfo, Immunohistochemical expression analysis of the human interferon-inducible gene IFI16, a member of the HIN200 family, not restricted to hematopoietic cells, J. Interferon Cytokine Res. 22 (2002) 815-821.

[15] W. Wei, C.J. Clarke, G.R. Somers, K.S. Cresswell, K.A. Loveland, J.A. Trapani, R.W. Johnstone, Expression of IFI 16 in epithelial cells and lymphoid tissues, Histochem. Cell Biol. 119 (2003) 45-54.

[16] F. Gugliesi, M. Mondini, R. Ravera, A. Robotti, M. de Andrea, G. Gribaudo, M. Gariglio, S. Landolfo, Up-regulation of the interferon-inducible IFI16 gene by oxidative stress triggers p53 transcriptional activity in endothelial cells, J. Leukoc. Biol. 77 (2005) 820-829.

[17] R. Raffaella, D. Gioia, M. De Andrea, P. Cappello, M. Giovarelli, P. Marconi, R. Manservigi, M. Gariglio, S. Landolfo, The interferon-inducible IFI16 gene inhibits tube morphogenesis and proliferation of primary, but not HPV16 E6/E7-immortalized human endothelial cells, Exp. Cell Res. 293 (2004) 331-345.

[18] M. Mondini, M. Vidali, M. De Andrea, B. Azzimonti, P. Airo, R. D'Ambrosio, P. Riboldi, P.L. Meroni, E. Albano, Y. Shoenfeld, M. Gariglio, S. Landolfo, A novel autoantigen to differentiate limited cutaneous systemic sclerosis from diffuse cutaneous systemic sclerosis: the interferon-inducible gene IFI16, Arthritis Rheum. 54 (2006) 3939-3944.

[19] M. Mondini, M. Vidali, P. Airo, D.E.A. M, P. Riboldi, P.L. Meroni, M. Gariglio, S. Landolfo, Role of the Interferon-Inducible Gene IFI16 in the Etiopathogenesis of Systemic Autoimmune Disorders, Ann. N Y Acad. Sci. 1110 (2007) 47-56.

[20] P. Hakansson, D. Segal, C. Lassen, U. Gullberg, H.C. Morse, 3rd, T. Fioretos, P.S. Meltzer, Identification of genes differentially regulated by the P210 BCR/ABL1 fusion oncogene using cDNA microarrays, Exp. Hematol. 32 (2004) 476-482.

[21] M. De Andrea, D. Gioia, M. Mondini, B. Azzimonti, F. Reno, G. Pecorari, V. Landolfo, M. Tommasino, R. Accardi, C. Herold-Mende, S. Landolfo, M. Gariglio, Effects of IFI16 overexpression on the growth and doxorubicin sensitivity of head and neck squamous cell carcinoma-derived cell lines, Head Neck 29 (2007) 835-844.

[22] N. Fujiuchi, J.A. Aglipay, T. Ohtsuka, N. Maehara, F. Sahin, G.H. Su, S.W. Lee, T. Ouchi, Requirement of IFI16 for the maximal activation of p53 induced by ionizing radiation, J. Biol. Chem. 279 (2004) 20339-20344.

[23] Y. Zhang, R.D. Howell, D.T. Alfonso, J. Yu, L. Kong, J.C. Wittig, C.J. Liu, IFI16 inhibits tumorigenicity and cell proliferation of bone and cartilage tumor cells, Front. Biosci. 12 (2007) 4855-4863.

[24] H. Xin, J. Curry, R.W. Johnstone, B.J. Nickoloff, D. Choubey, Role of IFI 16, a member of the interferon-inducible p200-protein family, in prostate epithelial cellular senescence, Oncogene 22 (2003) 4831-4840.

[25] B. Azzimonti, M. Pagano, M. Mondini, M. De Andrea, G. Valente, G. Monga, M. Tommasino, P. Aluffi, S. Landolfo, M. Gariglio, Altered patterns of the interferon-

inducible gene IFI16 expression in head and neck squamous cell carcinoma: immunohistochemical study including correlation with retinoblastoma protein, human papillomavirus infection and proliferation index, Histopathology 45 (2004) 560-572.

[26] P.R. Twentyman, M. Luscombe, A study of some variables in a tetrazolium dye (MTT) based assay for cell growth and chemosensitivity, Br. J. Cancer 56 (1987) 279-285.

[27] Aksamit RR, Falk W, Leonard EJ. Chemotaxis by mouse macrophage cell lines. *J Immunol*. 1981;126:2194 –2199.

[28] P. Caposio, F. Gugliesi, C. Zannetti, S. Sponza, M. Mondini, E. Medico, J. Hiscott, H.A. Young, G. Gribaudo, M. Gariglio, S. Landolfo, A novel role of the interferon-inducible protein IFI16 as inducer of proinflammatory molecules in endothelial cells, J. Biol. Chem. 282 (2007) 33515-33529.

[29] N.C. Kirkiles-Smith, M.J. Harding, B.R. Shepherd, S.A. Fader, T. Yi, Y. Wang, J.M. McNiff, E.L. Snyder, M.I. Lorber, G. Tellides, J.S. Pober. Development of a humanized mouse model to study the role of macrophages in allograft injury. Transplantation 87 (2009) 189-197.

[30] S. Ninck, C. Reisser, G. Dyckhoff, B. Helmke, H. Bauer, C. Herold-Mende, Expression profiles of angiogenic growth factors in squamous cell carcinomas of the head and neck, Int. J. Cancer 106 (2003) 34-44.

[31] M. Ouchi, T. Ouchi, Role of IFI16 in DNA damage and checkpoint, Front. Biosci. 13 (2008) 236-239.

[32] F. Alimirah, J. Chen, F.J. Davis, D. Choubey, IFI16 in human prostate cancer, Mol Cancer Res. 5 (2007) 251-259.

[33] L. Hertel, S. Rolle, M. De Andrea, B. Azzimonti, R. Osello, G. Gribaudo, M. Gariglio, S. Landolfo, The retinoblastoma protein is an essential mediator that links the interferon-inducible 204 gene to cell-cycle regulation, Oncogene 19 (2000) 3598-3608.

[34] M. Kelly, J.M. Hwang, P. Kubes, Modulating leukocyte recruitment in inflammation, J Allergy Clin. Immunol. 120 (2007) 3-10.

[35] K. Ley, C. Laudanna, M.I. Cybulsky, S. Nourshargh, Getting to the site of inflammation: the leukocyte adhesion cascade updated, Nat. Rev. Immunol. 7 (2007) 678-689.

[36] J. Martin, S. Collot-Teixeira, L. McGregor, J.L. McGregor, The dialogue between endothelial cells and monocytes/macrophages in vascular syndromes, Curr. Pharm. Des. 13 (2007) 1751-1759.

[37] J.E. Talmadge, M. Donkor, E. Scholar, Inflammatory cell infiltration of tumors: Jekyll or Hyde, Cancer Metastasis Rev. 26 (2007) 373-400.